ORGANOMETALLICS
Article
pubs.acs.org/Organometallics

Multinuclear Magnetic Resonance Spectroscopy and Density Function Theory Calculations for the Identification of the Equilibrium Species in THF Solutions of Organometallic Complexes Suitable As Electrolyte Solutions for Rechargeable Mg Batteries

Nir Pour, Yossi Gofer, Dan T. Major, Keren Keinan-Adamsky, Hugo E. Gottlieb, and Doron Aurbach*

Department of Chemistry and the Lise Meitner-Minerva Center of Computational Quantum Chemistry, Bar-Ilan University, Ramat-Gan 52900, Israel

Ⓢ *Supporting Information*

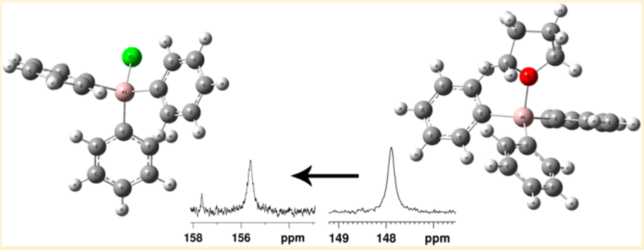

ABSTRACT: We present a multinuclear nuclear magnetic resonance (NMR) and density functional theory (DFT) study of electrolyte solutions based on organometallic complexes with aromatic ligands. These solutions constitute a unique electrolyte family possessing a wide electrochemical window, making them suitable for rechargeable magnesium batteries. In our previous study we identified equilibrium species in the solutions based on a combination of Raman spectroscopy and single-crystal XRD analyses,[1] and herein we extend our studies to include multinuclear NMR analyses. These solutions are comprised of the metathesis reaction products of $MgCl_{2-x}Ph_x$ and $AlCl_{3-y}Ph_y$ in various proportions, in THF. In principle, these reactions involve the exchange of ligands between the magnesium and the aluminum based compounds, forming ionic species and neutral molecules, such as $Mg_2Cl_3^+\cdot 6THF$, $MgCl_2\cdot 4THF$ and $AlCl_{4-y}Ph_y^-$ ($y = 0-4$). The identification of the solution phase species from the spectroscopic results is supported by spectral analyses of specially synthesized reference compounds and DFT quantum-mechanical calculations. The current approach reveals new aspects about the NMR shift of the organometallic complexes and, in particular, facilitates differentiation between ionic and neutral species.

INTRODUCTION

In the early 2000s, we presented the first prototype of a rechargeable magnesium battery.[2] This battery was realized largely because of the development of novel complex organometallic solutions of magnesium salts of the nominal formula $R_xMgCl_{2-x}\, R'_yAlCl_{4-y}^-$ (R, R′ = *n*-butyl and/or ethyl, $x = 0-2$, $y = 0-4$) in THF. The standard solution was selected to be the product of the metathesis reaction between $MgBu_2$ and $AlCl_2Et$ at a ratio of 1:2 forming, technically, $Mg(AlCl_2BuEt)_2$. This solution displayed favorable electrochemical characteristics, with an electrochemical stability window of ~2.2 V (vs Mg), specific conductivity of a few $10^{-3}\ \Omega^{-1}\ cm^{-1}$, and magnesium electrodeposition at 100% Coulombic efficiency. Nonetheless, such organometallic solutions suffer from a limited stability window, which hampers the possibility to couple the Mg anode with high voltage cathodes. It was shown that the weakest link that limits the oxidation stability is a carbon−aluminum bond that breaks electrochemically through a β-H-elimination.[3,4] Thus, we theorized that replacing the aliphatic ligands with phenyl, for which β-hydrogen elimination is impossible, will lead to significantly more robust organometallic complexes.

This new family of solutions is comprised of the metathesis reaction products of $MgCl_{2-x}Ph_x$ and $AlCl_{3-y}Ph_y$ in different proportions, in THF. These reactions involve the exchange of ligands between the magnesium and the aluminum based compounds, forming ionic species and neutral molecules, such as $Mg_2Cl_3^+\cdot 6THF$, $MgCl_2\cdot 4THF$ and $AlCl_{4-y}Ph_y^-$ ($y = 0-4$). These electrolytes will henceforth be referred to as "APC". The electrochemical stability of these solutions was measured by cyclic voltammetry and found to display a window of ~3.3 V (vs Mg),[1] proving that the basic hypothesis is correct.

In a previous paper[1] we presented a comprehensive analytical work, identifying nearly all the species existing in these solutions. In the current article we focus on multinuclear NMR studies in conjunction with DFT calculations, to complement the previous analyses of the organometallic complexes in THF. This combined approach allows identification of the entire range of species existing in the solutions (with the exception of trace compounds). In particular, we successfully differentiate between charged and neutral molecules. The excellent agreement between the calculated spectra and the trends obtained empirically resulted in the complete determination of the solutions composition.

Received: September 7, 2012

RESULTS AND DISCUSSION

Since the multinuclear NMR analysis provides vast amounts of information, we found it logical to divide it into two sections, namely, ^{13}C and ^{27}Al NMR. The integration of the data gained from ^{13}C and ^{27}Al NMR provides detailed information on the composition of the Al-based compounds. Thus, the current work, which identifies Al-based compounds, in combination with our previous identification of the remaining species employing Raman spectroscopy, forms a complete picture of the composition of this novel family of solutions.

DFT Calculated and Measured ^{13}C NMR. Previous ^{13}C, ^{1}H, ^{27}Al and ^{25}Mg NMR analyses revealed that the information extractable is restricted to the Al coordination number, i.e., the number of organic vs inorganic ligands.[4−7] In fact, very little could be gained from ^{13}C, ^{1}H and ^{25}Mg NMR analyses. One important limitation of the ^{27}Al NMR spectra is that the Cl and THF ligands affect the chemical shift in a similar manner. Thus, with the widths of the typical spectra it was impossible to differentiate between several pairs of molecules possessing the same number of phenyl groups, yet a different THF and Cl composition, e.g., $AlPh_3{\cdot}THF$ and $AlClPh_3^-$. In such cases, the different types of composition reflect neutral (THF) vs ionic molecules (Cl). Interestingly, the DFT calculations results for the ^{13}C NMR revealed coherent chemical-shift differences between such pairs of neutral and ionic species, which allowed, for the first time, to distinguish between them.

As was described in the previous account, correct selection of the basis-set and the reliability of the calculated molecule structures and their reconstructed spectra were ascertained by comparison between empiric and calculated data for selected pure compounds.

Table 1 below displays all the phenyl-ligand bearing Al and Mg species that can possibly exist in APC-type solutions and their corresponding ^{13}C NMR chemical shift obtained from the DFT calculations.

Table 1. Calculated ^{13}C NMR Peak Positions of *ipso*, *ortho*, *meta* and *para* Carbons of the Phenyl in the Al and Mg Species Using B3LYP/6-31+G(d,p)

	carbon [ppm (vs TMS)]			
molecule	*ipso*	*ortho*	*meta*	*para*
$AlCl_3Ph^-$	146.0	134.0	124.0	125.0
$AlCl_2Ph{\cdot}THF$	136.3	134.6	124.1	126.2
$AlCl_2Ph_2^-$	147.5	134.3	122.6	123.2
$AlClPh_2{\cdot}THF$	140.5	134.4	124.1	125.0
$AlClPh_3^-$	153.2	134.7	122.6	121.7
$AlPh_3{\cdot}THF$	144.3	135.7	124.1	124.8
$AlPh_4^-$	156.4	134.9	122.5	120.6
MgClPh	165.8	142.0	127.0	126.0

The phenyl ligands possess four sets of carbons that can be distinguished by NMR. Each of the carbons is affected differently by the Al core. The complete set of data for each of these carbons is listed below.

The peaks for phenylmagnesium chloride are also added. This molecule is the only organomagnesium species ever detected in our solutions under the limitation of our NMR and Raman spectroscopies. It is used to estimate the reliability of the DFT calculations of chemical shifts for our compounds. The calculated TMS ^{13}C NMR peak was used as a reference (see Experimental Section).

Several important results are presented in Table 1. (1) For each molecule (Al-based and Mg-based) the *ipso* carbon chemical shift is the largest, followed by the *ortho* carbon. (2) The *meta* and *para* carbons are always shifted significantly less than the *ipso* and *ortho* ones and show much smaller variability. (3) The *ipso* carbon shifts for the ionic species increase with increasing phenyl to Cl content ratio: ($AlCl_3Ph^-$) 146.0 < ($AlCl_2Ph_2^-$) 147.5 < ($AlClPh_3^-$) 153.2 < ($AlPh_4^-$) 156.4. (4) A similar trend is also observed for the *ortho* carbons, albeit with significantly smaller values. The more organic ligands (i.e., less Cl), the higher the chemical shift: ($AlCl_3Ph^-$) 134.0 < ($AlCl_2Ph_2^-$) 134.3 < ($AlClPh_3^-$) 134.7 < ($AlPh_4^-$) 134.9. (5) The *ipso* and the *ortho* shifts for the neutral molecules also followed the same trend, with a stronger effect for the *ipso* position. (6) The opposite trend is obtained for the chemical shifts of the *para* carbons, and a similar, although much weaker trend, for the *meta* carbons.

The results for MgClPh are also presented in Table 1. Its purpose was both for the validation of the correlation between the calculated spectra and the empirical data, and to serve as an identifier for phenyl ligand containing species in case they exist in the solution. The data show important features: The whole set of peaks appear with appreciably higher chemical shifts, the *ipso* carbon having the highest shift and the *para* the lowest. Compared to the equivalent carbons on the Al species, the *para* and *meta* carbon shifts are very close (difference of 2−3 ppm). However the *ortho* and *ipso* shift is much higher, as expected on the basis of the higher electropositivity of Mg and the ^{13}C NMR date reported in the literature for organo-phenyl compounds.[8]

The DFT calculated ^{13}C NMR data for the above species suggests that a reliable database compiling the related experimental data may be utilized for spectroscopic identification of the various species in the family of APC solutions. Specifically, the chemical shifts obtained from the calculations suggest that reliable identification of the relevant solution species can be realized by using a proper library of the *ipso* and *para* NMR peak shifts as they prove to be species specific. This feature adds cross-measurement certainty to Raman spectroscopy, as described in the previous paper. Moreover, the *ipso* chemical shifts complement the capability, unattained by Raman spectroscopy, to differentiate between the "equivalent" neutral versus anionic pairs (neutral and anionic species containing the same number of phenyl ligands).

Comparison of the *para*, *meta* and *ortho* carbon shifts for the ionic and neutral molecules with identical number of phenyl groups reveals that their chemical shifts are nearly indistinguishable. For example, the chemical shift for the *ortho* carbon in $AlCl_2Ph_2^-$ is 134.3 ppm, whereas for the corresponding "equivalent" neutral molecule, $AlClPh_2{\cdot}THF$, the shift is 134.4 ppm. This phenomenon has been demonstrated previously[5] and is rationalized on the basis of the similar effect THF and Cl have on the NMR chemical shifts of the phenyl *para*, *meta* and *ortho* carbons. In contrast, the *ipso* carbon shifts exhibit unique and significant differences between the neutral and ionic "equivalent" pairs. The shift for $AlPh_3{\cdot}THF$ is 144.3 ppm, while for its "equivalent" ionic pair, $AlClPh_3^-$, it is 153.2 ppm: a difference of 8.9 ppm. For the other two pairs, $AlCl_2Ph_2^-$/$AlClPh_2{\cdot}THF$ and $AlCl_3Ph^-$/$AlCl_2Ph{\cdot}THF$, the shift differences are 7.0 and 9.7 ppm, respectively.

As displayed by the DFT calculation, each of the *para*, *meta*, *ortho* and *ipso* carbons has a range of chemical shifts centered around a unique value. These shifts are very informative as they depend in a consistent manner on the nature of the molecule (ionic, neutral, number of phenyl groups, etc.). Experimental ^{13}C NMR limitations preclude the use of this tool to differentiate between the different molecules through the *para* and *meta* peaks. Fortunately, the spectral features for the *ortho* and *ipso* carbons were obtained with sufficient quality to allow distinguishing between the complexes.

We measured the ^{13}C NMR spectra for a wide variety of THF solutions containing either single, known compounds or the reaction products of MgClPh with $AlCl_{3-x}Ph_x$ The empirical shifts obtained followed the expected trend (from the DFT calculated spectra): the higher the number of phenyl ligands on the aluminum, the larger the chemical shift (downfield).

Because of the lack of essential literature data on the spectral properties of many of the relevant molecules, we first compiled a spectral database by measuring the multinuclear NMR spectra for solutions containing known compounds. The empirical data was also correlated with the DFT calculated spectra. In a few cases, where it was possible, pure compound solutions in THF were measured for the library. In other cases, where a great excess of a specific molecule was unequivocally identified by other spectroscopies (^{27}Al NMR, Raman, SC-XRD), the ^{13}C spectrum was also measured for the same purpose. In all other cases the measured spectrum had to be carefully analyzed, as it contained an equilibrium mixture of several molecules at an unknown molar ratio.

Figure 1 presents the spectrum obtained in the spectral region between 120−170 ppm. In this region there are number of significant peaks that are related to the different carbons of the phenyl group. The peaks at 123.9, 125.5, 141, and 170 ppm correspond to the *para*, *meta*, *ortho* and *ipso* position, respectively. Table 2 presents a comparison between the ^{13}C NMR chemical shifts obtained with DFT and the measured ones for MgClPh. In both cases we used the TMS ^{13}C NMR peak position as the reference for the comparison (see Experimental Section).

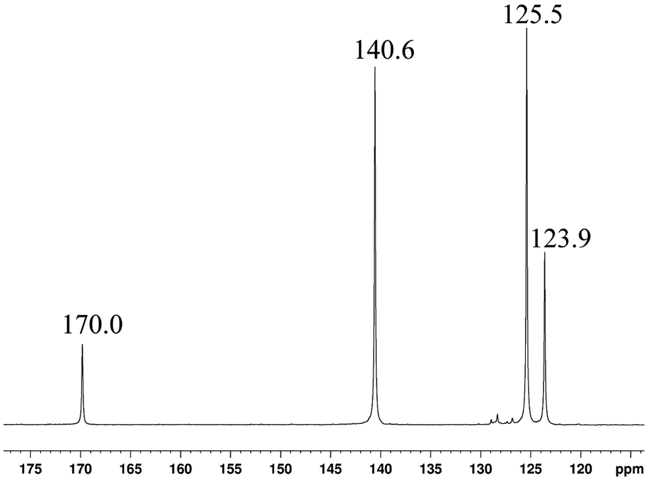

Figure 1. ^{13}C NMR spectrum of 0.5 M MgClPh in THF (shift vs TMS).

Table 2 shows that once an appropriate reference data point is selected, there is a very good correlation between the DFT results and the measured ones. The computed trend is in reasonable agreement with the observed trend, and the chemical shifts are of similar magnitude. Such a correlation was also obtained in all the comparisons between the ^{13}C NMR spectra obtained from the DFT and the measured ones (vide infra).

Table 2. Calculated (B3LYP/6-31+G(d,p)) and Measured ^{13}C NMR Comparison of Phenyl Carbons in MgClPh (Shift vs C3 of THF)

	MgClPh ^{13}C NMR [ppm (vs TMS)]			
$C_{position}$	*ipso*	*ortho*	*meta*	*para*
calc	165.8	142.0	127.0	126.0
measured	170.0	140.6	125.5	123.9
Δ	4.2	−1.4	−1.5	−2.1

$MgPh_2$ has frequently been used as a reactant in electrolyte synthesis.[1] the ^{13}C spectrum for this molecule was indistinguishable from the one obtained for MgClPh (see Figure S1, Supporting Information). Thus, NMR measurements are not practical for differentiation between MgClPh and $MgPh_2$, and only elemental analysis achieved clear identification. (Raman measurements were also inadequate in this respect because of strong fluorescence interfering with the analysis).

Figure 2 displays the ^{13}C NMR spectrum for $AlPh_3$·THF. This is one of the two molecules we were able to obtain as a single component in THF and thus was valuable for the compilation of a reliable spectral database. Raman spectroscopy for the solution proved that this solution contains only one Al-based specie, and ^{1}H NMR proved that this molecule is $AlPh_3$·THF (and not $AlClPh_3^-$).[1]

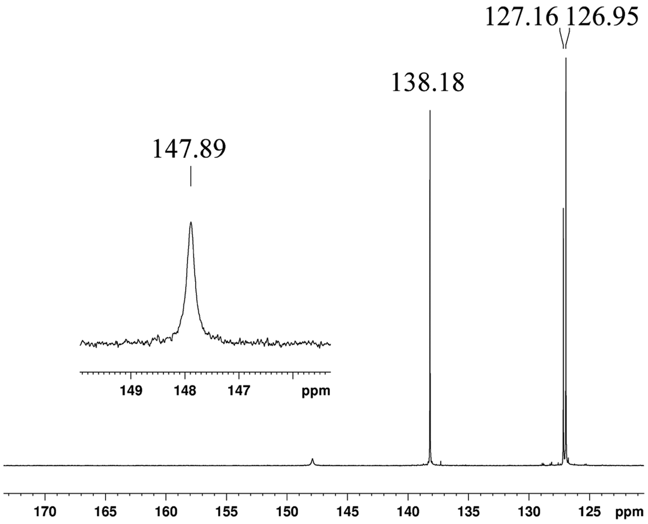

Figure 2. ^{13}C NMR spectrum of 0.25 M $AlPh_3$·THF in THF (shift vs TMS).

The spectrum of this molecule was very valuable as it was the first verified neutral molecule in of the APC family to be identified.

Figure 2 presents the 120−160 ppm region and a magnification of the 150 ppm region (insert). There are a number of significant peaks that relate to the different carbons on the phenyl group. The peaks at 126.9, 127.1, 138.2, and 147.9 ppm, correspond to the *para*, *meta*, *ortho* and *ipso* carbons, respectively. As with the case of MgClPh, a constantly increasing shift was also observed in the DFT calculation presented in Table 1.

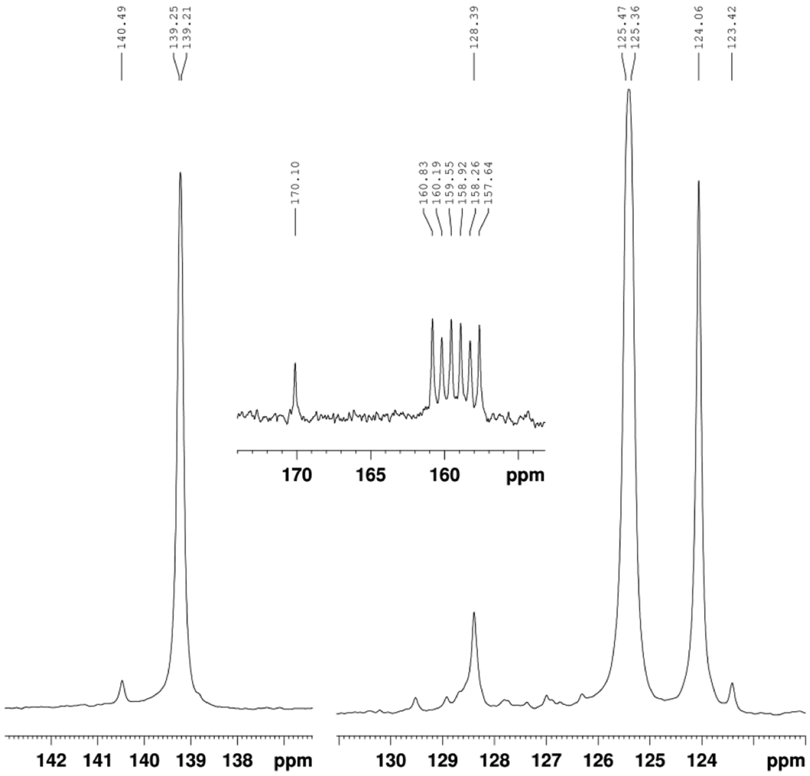

Figure 3. ^{13}C NMR spectrum of APC 1−4 (0.25 M $AlCl_3$ and 1 M MgClPh) in THF. Insert: Magnified 160−175 ppm region (shift vs TMS).

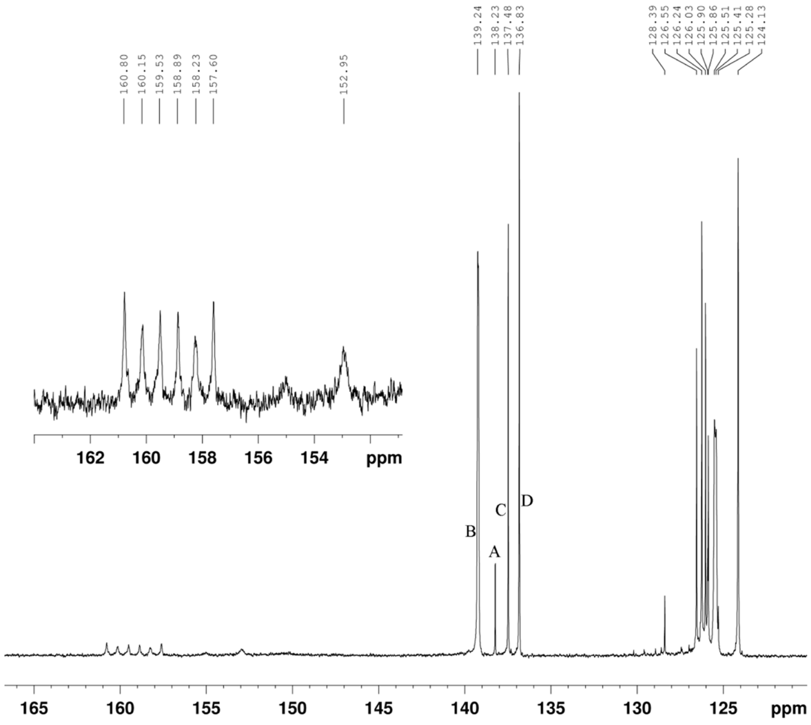

Figure 4. ^{13}C NMR spectrum of 0.4 M APC (0.4 M $AlCl_3$ and 0.8 M MgClPh) in THF (shift vs TMS).

The spectra presented below were measured in various solutions, in which only partial molecular identifications were obtained previously from Raman spectroscopy. In addition to the partial knowledge regarding the solution chemistry, all these solutions are expected to include multiple equilibrium species. Because of the lack of resolution and the richness in peaks, in most cases it was not possible to differentiate between the *para* and *meta* carbon peaks of the different species. Therefore, our analysis has to focus on the *ipso* and *ortho* carbons. Unfortunately, the *ipso* carbon signal was usually very weak and in some cases unobservable. Figure 3 displays the spectrum of APC 1−4; this solution was synthesized from 0.25 M $AlCl_3$ and 1 M MgClPh as described in the Experimental Section.

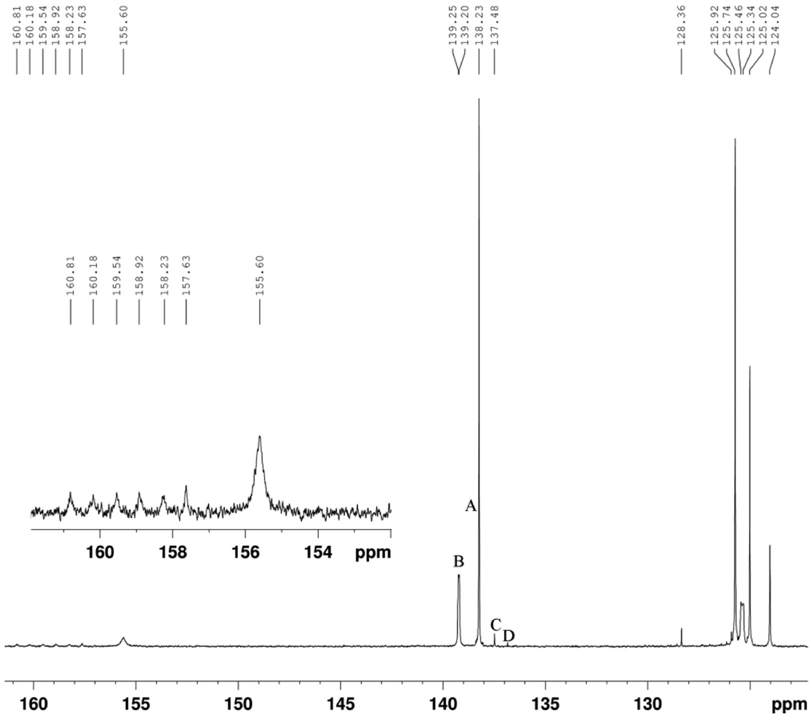

Figure 5. ^{13}C NMR spectrum of 0.4 M APC + 0.8 M LiCl (0.4 M AlCl3 and 0.8 M MgClPh + 0.8 M LiCl) in THF (shift vs TMS).

From the Raman spectrum of this solution we identified the main Al-species in this solution to be $AlPh_4^-$.

As one can see, this spectrum is much richer in peaks, as expected from solution containing several species in equilibrium. Some of the species in this case, however, have very low concentration. Figure 3 presents the 120−170 ppm region and magnifications of two important regions. In this spectrum we can see the peaks already presented in Figure 1, related to MgClPh (at ∼123, ∼125.5, ∼141, and 170 ppm). The presence of MgClPh and its associated peaks is expected, as this solution was synthesized with an excess of MgClPh. Apart for the features associated with this already identified molecule, four new peaks are clearly seen, at 124.0, 125.4, 139.2, and 159.0 ppm. On the basis of the information obtained from Raman spectroscopy, we ascribe these peaks to the *para*, *meta*, *ortho* and *ipso* carbons of $AlPh_4^-$, respectively. A weak peak is also observed at 128.4 ppm. This peak corresponds to benzene.[9] Benzene is a common breakdown product of these organometallic molecules; therefore, the presence of its traces in these solutions is not unexpected. A unique feature in the spectrum is the location of the *ipso* carbon, at 160 ppm. Because of its direct bond to ^{27}Al, it clearly displays the 6-fold splitting, resulting from the spin coupling with the aluminum nucleus. For $AlPh_4^-$ these splittings are particularly visible because of the high symmetry of the molecule. This splitting is not seen in the *ipso* carbon features of the other molecules ($AlClPh_3^-$, $AlCl_2Ph_2^-$ etc.). Because of lower symmetry of these species, the peaks are too weak and broad to show the fine splitting details.

Figure 4 presents the ^{13}C NMR for 0.4 M APC solution (this solution was synthesized from 0.4 M $AlCl_3$ and 0.8 M MgClPh in THF). From previous Raman spectroscopy, it was established that this solution contains a wide range of Al species.[1]

When examining the peaks associated with the *ortho* carbons, in the 135−140 ppm region, it can be determined that there are 4 different species in the solution (marked A to D). On the basis of the understanding gained to date[4,10] and on the DFT results, these peaks can be assigned as follows: 136.8 ppm to $AlCl_3Ph^-$, 137.5 ppm to $AlCl_2Ph_2^-$, 138.2 ppm to $AlClPh_3^-$ (see Figure 2) and 139.2 ppm to $AlPh_4^-$ (see Figure 3). On the basis of the *ipso* carbon features, which will be thoroughly discussed later, and supported by ionic conductivity measurements, we conclude that these species are all ionic. In Figure 4 one can also observe the 6-fold spin coupled splitting of the $AlPh_4^-$ peak at 160 ppm. Although weak, but still discernible, one can identify the *ipso* carbon peaks of $AlClPh_3^-$ at 155 ppm, and the *ipso* carbon peaks for $AlCl_2Ph_2^-$ and $AlCl_3Ph^-$ at ∼153 ppm.

Figure 5 presents the ^{13}C NMR spectrum for 0.4 M APC solution containing 0.8 M LiCl (LiCl is added as electrochemical ionic additive[1]). On the basis of Raman analysis, this solution was determined to contain $AlClPh_3^-$ that is the main Al-based species. Figure 5 displays the measured ^{13}C NMR spectrum of 0.4 M APC solution + 0.8 M LiCl in THF.

In the 140 ppm region, the same 4 peaks presented in Figure 4 are also observed. However, in this solution, the peak at 138.2 ppm (A) is much stronger than the other three. This peak is assigned to the *ortho* carbon for $AlClPh_3^-$. From the peak integration it is evident that this molecule exists in excess. Comparison between this spectrum and that for $AlPh_3 \cdot THF$ in Figure 2 reveals the difference between the chemical shifts for the “equivalent” ionic and the neutral molecules. A unique and significant spectral difference is seen, as predicted from the DFT calculations, in the *ipso* carbon chemical shift, in the 150 ppm region. From Figure 2, it is found that the *ipso* carbon peak for $AlPh_3 \cdot THF$ is at 147.9 ppm, whereas the “equivalent” anion, $AlClPh_3^-$, shows the *ipso* carbon peak at 155.6 ppm. The experimental difference in position between these two peaks is about 9 ppm, close to the DFT results that predicted a difference of 10 ppm. These results complete the identification of the variety of species present in APC-type solutions by ^{13}C NMR, including the possibility to distinguish between neutral and ionic molecules. Further corroboration of the peak assignments for the spectra in Figures 3, 4, and 5 are given in the Figures S2−S4 (Supporting Information).

Two practical conclusions can be derived from meticulous examination of the empirical ^{13}C NMR spectra for the APC-family of organometallic complex solutions: (1) The peak position of the *ipso* carbons can be utilized to distinguish between neutral and ionic molecules, otherwise equivalent both in ^{27}Al NMR and Raman spectroscopy. (2) The peaks position of the *ortho* carbon can be used to determine the number of phenyl ligands bound to the aluminum.

Table 3 summarizes the measured ^{13}C NMR peaks positions of the *ipso* and *ortho* carbons as obtained from Figures 3, 4, 5 and Figures S2−S4 (Supporting Information). This is used in the following tables for the comparison between the measured and the calculated peaks positions.

Table 3. Measured ^{13}C NMR Peaks Positions of *ipso* and *ortho* Carbons of the Phenyl in the Al and Mg Species

molecule	carbon [ppm (vs TMS)]	
	ortho	*ipso*
MgClPh	140.6	170.0
$MgPh_2$	140.6	170.0
$AlPh_4^-$	139.2	159.0
$AlClPh_3^-$	138.2	155.6
$AlCl_2Ph_2^-$	137.3	152.9
$AlCl_3Ph^-$	136.6	152.9
neutral	n/a	n/a
$AlPh_3\cdot THF$	138.2	147.9

The DFT results presented at the beginning of the paper predicted that the more phenyl groups attached to the Al, the higher the ppm value of the *ipso* and *ortho* carbon. Moreover, the DFT calculations predicted that the corresponding chemical shifts for the organomagnesium species will be downfield. It can be seen from Table 3 that the trends in the measured chemical shifts for all the above organometallic compounds follow those predicted by the DFT calculations.

In order to highlight the correlation between the DFT calculations results and the measured spectra, Table 4 compares the chemical shift (vs TMS) of a specific carbon type (*ortho*, *ipso* of the ionic molecules and *ipso* of the "equivalent" neutral molecules) obtained from the DFT calculations and the ^{13}C NMR measurements.

Table 4. Calculated (B3LYP/6-31+G(d,p)) and Measured ^{13}C NMR Chemical Shifts (vs TMS) of *ipso* and *ortho* Carbons of the Al-Species

	ionic molecules: *ortho* carbon			
	$AlPh_4^-$	$AlClPh_3^-$	$AlCl_2Ph_2^-$	$AlCl_3Ph^-$
calculated	134.7	134.7	134.3	134
measured	139.2	138.2	137.3	136.6
Δ	4.5	3.5	3	2.6
	ionic molecules: *ipso* carbon			
	$AlPh_4^-$	$AlClPh_3^-$	$AlCl_2Ph_2^-$	$AlCl_3Ph^-$
calculated	155.4	153.2	147.5	146.0
measured	159	155.6	152.9	152.9
Δ	3.6	2.4	5.4	6.9
	neutral molecules: *ipso* carbon			
	$AlPh_3\cdot THF$	$AlClPh_2\cdot THF$	$AlCl_2Ph\cdot THF$	
calculated	144.3	140.5	136.3	
measured	147.9	n/a	n/a	

From Table 4 it can clearly be seen that the DFT calculations reproduce fairly well the ^{13}C NMR shifts for the phenyl Mg and Al organometallic compounds. In some cases, the difference between the calculated values and the measured are as low as 2.6 ppm.

DFT Calculated and Empirical ^{27}Al NMR. Previous studies of a homologue series of aliphatic organometallic complexes,[10] and related work,[11−14] have shown that ^{27}Al NMR contains invaluable structural information. In many cases it can be used to shed light on structural and chemical aspects of aluminum-based molecules. This is despite the quadrupolar ^{27}Al nucleus,[6,7] which causes peak broadening. It has been shown,[15] as a rule of thumb, that the coordination number of the aluminum core atom is the primary influencing parameter on the chemical shift. To a lesser degree, but still significantly, the ligand's nature influences the chemical shift in an additive and predictable manner: while inorganic ligands, like Cl^-, drive the chemical shift upfield, organic ligands drive the chemical shift downfield. In this respect, it was previously shown that highly polar donor ligands, such as THF, influence the chemical shift in an identical manner to Cl^-. These phenomenological features combined with DFT calculations and Raman spectroscopy facilitate complete identification of all species in these complex, multicomponent organometallic equilibrium solutions.

In contrast, the ^{25}Mg NMR spectra are much less informative and usually too broad and weak to be of help in structural determination. In addition, the ^{25}Mg NMR spectra demonstrate much smaller chemical shift variations.

Table 5 lists the ^{27}Al NMR shifts obtained from the DFT calculations (B3LYP/6-31+G(d,p)) for the various molecules, as described before. The peak for $AlCl_3THF$ was taken as a reference.

Table 5. Calculated ^{27}Al NMR Chemical Shifts for the Al Species Using B3LYP/6-31+G(d,p)

DFT calculated ^{27}Al NMR shift	
molecule	chemical shift [ppm]
$AlCl_3\cdot THF$	0.0
$AlCl_4^-$	0.2
$AlCl_3Ph^-$	17.5
$AlCl_2Ph\cdot THF$	19.4
$AlCl_2\ Ph_2^-$	32.3
$AlClPh_2\cdot THF$	36.4
$AlClPh_3^-$	43.9
$AlPh_3\cdot THF$	52.1
$AlPh_4^-$	28.3

The results of the DFT calculations listed in Table 5 show a clear trend in the chemical shifts. As was shown before, the chemical shift depends on the $Ph:Cl^-$ ratio for all the tetracoordinated molecules. Moreover, THF as a ligand influences the chemical shift in a qualitatively similar way to the inorganic ligand, but quantitatively different. As a general rule, it can be said that the higher the $Ph:Cl^-$ ratio, the higher the chemical shift for these tetracoordinated organometallic Al based coordination species.

Interestingly, $AlPh_4^-$ is an outlier in this respect. This molecule's ^{27}Al NMR peak appears at a significantly lower ppm than expected on the basis of the constantly increasing chemical shift with increasing number of phenyl ligands. This phenomenon is still not fully understood. However, since this phenomenon is both predicted by the DFT calculations and obtained in the NMR measurement, it suggests that it reflects subtle changes in the electronic structure of the tetracoordinated, all organic ligand, molecule. It is important to note here that the very same phenomenon was revealed for the series of organo-halo aliphatic (ethyl, butyl) compounds, the DCC family of electrolytes.[15]

Also, the differences in the chemical shifts obtained for "equivalent" neutral ionic pairs, show a constant trend: the chemical shift for the neutral molecule is usually higher than that of its "equivalent" anionic. For example, the ^{27}Al peak for $AlCl_3Ph^-$ is 17.5 ppm, while its neutral "equivalent", $AlCl_2Ph·THF$ is at 19.4 ppm. The pair $AlCl_3·THF$ and $AlCl_4^-$ is an exception to this trend, although the differences in the chemical shifts are exceedingly small. As will be shown later, most of the trends obtained above from the DFT calculations were observed in the measured spectra for the molecules that could be synthesized.

Figure 6 displays two ^{27}Al NMR spectra, (a) for 0.25 M $AlCl_3$ in THF and (b) APC 1−4.

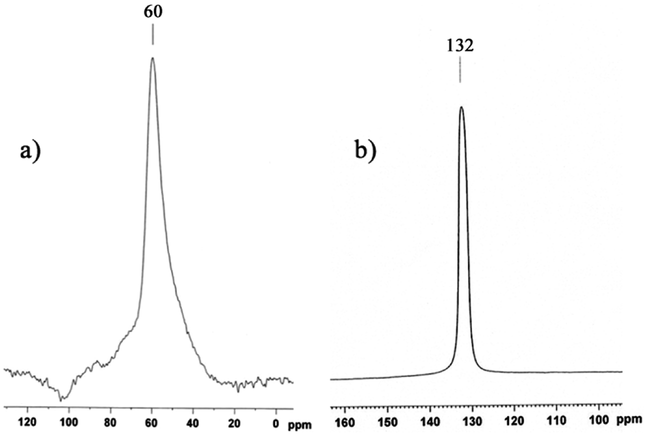

Figure 6. ^{27}Al NMR spectra of (a) 0.25 M $AlCl_3$ in THF and (b) APC 1−4 ($AlPh_4^-Mg_2Cl_3^+$ in THF).

0.25 M $AlCl_3$ in THF contains mainly the tetracoordinated $AlCl_3·THF$ and its measured NMR peak is at 60.4 ppm (Figure 6a).[6] Figure 6b, presents the ^{27}Al NMR spectrum for APC 1−4 solution. The ^{13}C NMR spectrum for the same solution was presented in Figure 3. The main Al species in this solution was proven to be $AlPh_4^-$. Thus the peak at 131.9 ppm is assigned to the $AlPh_4^-$. Both $AlPh_4^-$ and $AlCl_3·THF$ display sharp and strong peaks. Because of its high symmetry, $AlPh_4^-$ displays the sharpest and highest peak among all the current ^{27}Al NMR spectra.

Further confirmation of the existence of $AlPh_4^-$ in the APC 1−4 solution came from a complementary measurement of solid state ^{27}Al NMR. As was described in a previous paper,[1] crystals precipitated from APC 1−4 solutions were identified as $AlPh_4^-Mg_2Cl_3^+$ by SC-XRD. Figure 7 below presents the solid state ^{27}Al NMR spectrum of these crystals.

As in the case of the solution spectra, solid state ^{27}Al NMR for $AlPh_4^-$ shows very sharp peaks owing to its high symmetry.

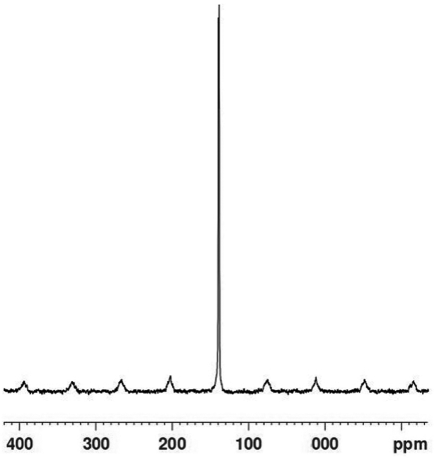

Figure 7. Solid-state ^{27}Al NMR spectrum of the $AlPh_4^-Mg_2Cl_3^+$.

All the other ^{27}Al NMR spectra display wider and weaker peaks, as presented in Figure 8, below.

The spectrum of $AlPh_3·THF$ in THF in Figure 8a exhibits a single peak at 142.3 ppm with a weak, but noticeable shoulder to the right, presumably associated with traces of the reactant $AlCl_3$. Figure 8b displays the spectrum obtained from the APC 2−1 solution. This solution was shown, on the basis of Raman and ^{13}C NMR (Figure S3, Supporting Information), to contain a mixture of $AlCl_3Ph^-$, $AlCl_4^-$ and $AlCl_3·THF$. The peak for $AlCl_3·THF$ can clearly be seen in the 60 ppm region.[6] The ^{27}Al NMR for $AlCl_4^-$ is reported to be located at around 102−108 ppm,[16] and thus it can be inferred that the wide peak at 102.5 ppm is a superposition of the two peaks associated with $AlCl_3Ph^-$ (~107.0 ppm, Figure S5, Supporting Information) and $AlCl_4^-$ (~100.0 ppm, Figure S5, Supporting Information). Figure 8c displays the spectrum obtained from 0.25 M APC, the standard working electrochemical solution. It was shown previously by Raman and ^{13}C NMR to contain a very wide array of species in equilibrium.[1] This spectrum is displayed in order to emphasize the difficulty in the analysis of these complex organometallic compounds solutions. Figure 8 illustrates the need for the combined work of multinuclear NMR and Raman spectroscopy, with the aid of high quality DFT calculations for the reliable peak associations. As can be seen in Figure 8, apart from two clearly identifiable peaks, the spectrum displays very wide and smeared overlapping features associated with a variety of species. Additional spectra are displayed in Figures S5 and S6 (Supporting Information) supporting the remaining peak assignments.

Table 6 summarizes and compares all the measured and DFT calculated ^{27}Al NMR peaks for the above organometallic compounds. For simplicity the NMR shifts in Table 6 are referenced to $AlCl_3$.

Interestingly, despite the relatively large difference between the calculated and the measured chemical shifts, the same general trend can be observed: more organic ligands attached to the Al results in a higher chemical shift. Also, the exception to the trend related to the $AlPh_4^-$ chemical shift is also predicted by the DFT calculations. Increasing the basis set with the B3LYP functional does not significantly change the chemical shifts. However, slightly better agreement with experiment is obtained with the mPW1PW91 functional with a larger basis set.[17,18] We note that calculating ^{27}Al chemical shifts is challenging for modern DFT methods,[19] although the errors

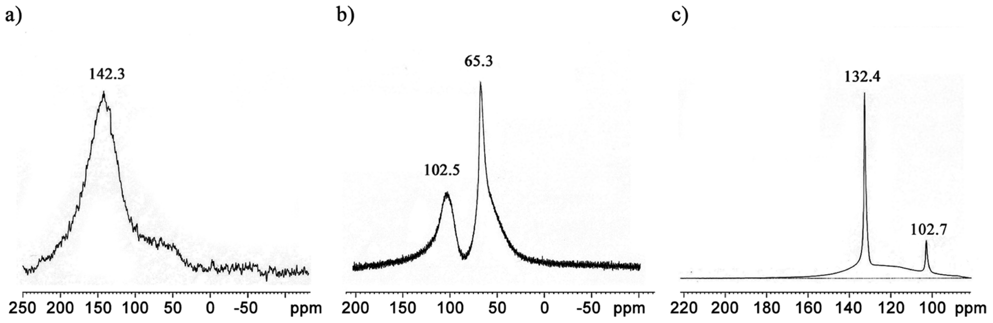

Figure 8. ^{27}Al NMR spectra of (a) 0.25 M $AlPh_3{\cdot}THF$, (b) APC 2−1 (0.25 M $AlCl_3$ + 0.125 M MgClPh), and (c) 0.25 M APC (0.25 M $AlCl_3$ + 0.5 M MgClPh). All spectra were measured in THF.

Table 6. Calculated and Measured ^{27}Al NMR Comparison of the Al-Species

		^{27}Al NMR (ppm vs $AlCl_3$)			
	$AlCl_4^-$	$AlCl_3Ph^-$	$AlCl_2Ph_2^-$	$AlPh_3{\cdot}THF$	$AlPh_4^-$
calculated (ppm)[a]	0.2	17.5	32.3	52.1	28.3
calculated (ppm)[b]	6.9	21.8	35.3	n/a	n/a
measured (ppm)	42−48	47.0	60.0	82.3	72.0

[a] B3LYP/6-31+G(d,p). [b] mPW1PW91/Aug-cc-pVTZ.

herein are somewhat larger than what is typically observed for ^{27}Al species. We also computed the $^1J(^{27}Al,^{13}C)$ coupling constants for $AlPh_4^-$. The computed value using mPWPW91/6-31+G(d,p) is 74.9 Hz (while the measured value from our experiments was 96.0 Hz), comparable to the computed value for Al(*t*-Bu)$_3$ of 76.3 Hz.[20] In spite of the significant differences between the calculated and the empirical results for the chemical shifts, the importance of the ^{27}Al NMR analysis to fully unravel the existing species of the metallic−organic solutions is demonstrated.

CONCLUSIONS

In this paper we completed the identification of the equilibrium species in the APC family of electrolyte solutions formed by reacting MgClPh and $AlCl_3$ in THF. Multinuclear NMR combined with Raman spectroscopy, elemental analysis and DFT calculations were utilized to carry out this complex endeavor. Both the Al and Mg based species, neutral and ionic, were identified, and their spectral features were reported. It was shown that for the complete elucidation of the various mixtures of equilibrium compounds, the combined use of ^{13}C, ^{27}Al NMR and Raman spectroscopic measurements is crucial. Each of the spectroscopic techniques is used for the identification of particular pieces of the complete picture, and only the combined work can lead to complete analysis. NMR, like Raman spectroscopy, is especially suited for the task of identifying the equilibrium solution species of these organometallic compounds under identical conditions to those exercised during the electrochemical measurements. The analysis of the APC electrolytic system is particularly important, as it is one of the most advanced electrolyte solutions for rechargeable magnesium batteries with operating voltage of up to 3 V. The spectroscopic methods and the spectral database obtained in this work can be valuable for the analysis of similar complexes and organometallic species in other fields, such as organic synthesis and polymerization catalysis.

EXPERIMENTAL SECTION

All the syntheses and electrochemical measurements were carried out under pure argon atmosphere (99.999%) in a M. Braun, Inc., glovebox (less than 1 ppm of water and oxygen).

Chemicals and Syntheses. All electrolyte solutions were synthesized according to the same basic procedure: First, $AlCl_3$ (Aldrich, anhydrous, 99.999%) in THF (Aldrich, 99.9%, less than 20 ppm water) solution was prepared in the desired concentration by very slow addition to the vigorously stirred solvent. Then, this solution was added dropwise to a predetermined quantity of 2 M phenylmagnesium chloride (MgClPh) solution in THF (Aldrich). Both reactions are very exothermic. The resulting solution was stirred for additional 16 h or more (at room temperature).

The family of electrolytes containing phenyl ligands in various proportions are referred to in this paper as "APC" (all phenyl complex). Electrolyte concentrations are reported in terms of the aluminum-based species concentration. If not indicated otherwise, the $AlCl_3$ to MgClPh ratio is 1:2. Thus, a 0.25 M APC solution is synthesized by reacting equal quantities of 0.25 M $AlCl_3$ and 0.5 M MgClPh in THF. The standard electrolyte, to which others are compared, is 0.25 M APC, as it exhibits favorable electrochemical properties. In cases where solutions were prepared with $AlCl_3$ and MgClPh at ratios other than 1:2, they are denoted as APC *m*:*n* solutions (*m* and *n* are the relative amounts of $AlCl_3$ and MgClPh, respectively). Unless otherwise noticed, the $AlCl_3$ concentration that was used in all of the solutions was 0.25 M.

Synthesis of $AlPh_3{\cdot}THF$ Reference Compound.[21] A 2 M THF solution of phenylmagnesium chloride (22.5 mmol) was slowly added to a 1.2 M solution of $AlCl_3$ (1.0 g, 7.5 mmol) in THF (6.25 mL) at 0 °C. The solution was then stirred for 14 h at rt, after which the solvent was removed under reduced pressure. The solid residue (mainly $MgCl_2$) was separated and removed by toluene extraction and centrifugation. The white powder left after toluene removal contained mainly $AlPh_3{\cdot}THF$ with less than 10% (molar) $MgCl_2$. NMR indicated a Ph:THF ratio of 3:1.[1]

$MgPh_2$ syntheses followed well-documented procedures.[22]

Nuclear Magnetic Resonance. NMR spectra of the solutions were measured with a Bruker DMX-600 spectrometer. Solutions of different concentrations and ratios of reagents in THF were measured in 8 mm NMR tubes without a deuterium lock. ^{13}C chemical shifts are reported in the figures relative to TMS. ^{27}Al chemical shifts are reported relative to external references: a solution of $AlCl_3$ in H_2O. All the measurements were performed at room temperature (25 ± 2 °C).

DFT Computations. All aluminum core geometry optimizations were performed at the B3LYP/6-31+G* level of theory.[23−25] Magnesium core geometry optimizations were done at the B3LYP/CEP-31+G* level in the gas-phase and in solution. The solvent (THF, $\varepsilon = 7.58$) was taken into account via the IEFPCM model.[26] Theoretical NMR spectra were calculated at the B3LYP/6-31+G(d,p) level in solution, as well as with the mPW1PW91 functional[27] in conjunction with the Aug-cc-pVTZ basis set.[28,29] For comparison between the calculated and the measured ^{13}C NMR, the peak position of the carbon in TMS (192.981 ppm as obtained from the DFT calculation) was used as a reference. All calculations were performed using Gaussian 09 package.[30]

■ ASSOCIATED CONTENT

Ⓢ Supporting Information

Supporting Figures S1−S6. This material is available free of charge via the Internet at http://pubs.acs.org.

■ AUTHOR INFORMATION

Corresponding Author

*Tel: 972-35318317. E-mail: Doron.Aurbach@biu.ac.il.

Notes

The authors declare no competing financial interest.

■ ACKNOWLEDGMENTS

Partial support for the work was obtained from the I-SAEF (Israel−US Strategic Alternative Energy Foundation) and from Pellion, Inc., USA.

■ REFERENCES

(1) Pour, N.; Gofer, Y.; Major, D. T.; Aurbach, D. *J. Am. Chem. Soc.* **2011**, *133* (16), 6270−6278.
(2) Aurbach, D.; Lu, Z.; Schecter, A.; Gofer, Y.; Gizbar, H.; Turgeman, R.; Cohen, Y.; Moshkovitz, M.; Levi, E. *Nature* **2000**, *407*, 724.
(3) Aurbach, D.; Gizbar, H.; Schechter, A.; Chusid, O.; Gottlieb, H. E.; Gofer, Y.; Goldberg, I. *J. Electrochem. Soc.* **2002**, *149*, A115.
(4) Gofer, Y.; Chusid, O.; Gizbar, H.; Vestfrid, Y.; Gottlieb, H. E.; Marks, V.; Aurbach, D. *Electrochem. Solid-State Lett.* **2006**, *9*, A257.
(5) Gizbar, H. *The Study of Non Aqueous Electrochemical Systems of Magnesium*. Ph.D. Thesis, Bar-Ilan University, 2006.
(6) Mizrahi, O. *Electrolyte Solutions for Rechargeable Magnesium Batteries*. M.Sc. Thesis, Bar-Ilan University, 2007.
(7) Ashby, E. C. *Q. Rev. Chem. Soc.* **1967**, *21*, 259.
(8) Sakamoto, S.; Imamoto, T.; Yamaguchi, K. *Org. Lett.* **2001**, *3*, 1793.
(9) Kalinowski, H. O.; Berger, S.; Braun, S. *Carbon-13 NMR Spectroscopy*; Wiley: New York, 1988.
(10) Vestfries, Y.; Chusid, O.; Goffer, Y.; Aped, P.; Aurbach, D. *Organometallics* **2007**, *26*, 3130.
(11) Benn, R. *J. Organomet. Chem.* **1987**, *333*, 169−180.
(12) Benn, R. *J. Organomet. Chem.* **1987**, *333*, 155−168.
(13) Benn, R. *Angew. Chem., Int. Ed. Engl.* **1986**, *25*, 861−881.
(14) Benn, R. *Angew. Chem., Int. Ed. Engl.* **1983**, *22*, 779−780.
(15) Gizbar, H.; Vestfrid, Y.; Chusid, O.; Gofer, Y.; Gottlieb, H. E.; Marks, V.; Aurbach, D. *Organometallics* **2004**, *23*, 3826−3831.
(16) Cerny, Z.; Machacek, J.; Casensky, B.; Kriz, O.; Tuck, D. G. *Inorg. Chim. Acta* **2000**, *300−300*, 556.
(17) Wiberg, K. B. *J. Comput. Chem.* **1999**, *20*, 1299−1303.
(18) Weitman, M.; Lerman, L.; Nudelman, A.; Major, D. T.; Gottlieb, H. E. *Tetrahedron* **2010**, *66*, 1465−1471.
(19) Wang, X.; Wang, C.; Zhao, H. *Int. J. Mol. Sci.* **2012**, *13*, 15420−15446.
(20) Wrackmeyer, B.; Klimkina, E. V. *Z. Naturforscher* **2008**, *63b*, 923−928.
(21) Chen, C. R.; Gau, H. M. *Acta Crystallogr.* **2008**, *E64*, m1381.
(22) Wotiz, J. H.; Hollongsworth, C. A.; Dessy, R. E. *J. Am. Chem. Soc.* **1956**, *78*, 1221.
(23) Becke, A. D. *J. Chem. Phys.* **1993**, *98*, 5648−5652.
(24) Lee, C.; Yang, W.; Parr, R. G. *Phys. Rev. B* **1988**, *37*, 785−789.
(25) Hehre, W. J.; Radom, L.; Schleyer, P. v. R.; Pople, J. A. *Ab Initio Molecular Orbital Theory*; John Wiley & Sons: New York, 1986.
(26) (a) Cance, M. T.; Mennucci, B.; Tomasi, J. *J. Chem. Phys.* **1997**, *107*, 3032. (b) Mennucci, B.; Tomasi, J. *J. Chem. Phys.* **1997**, *I*, 5151. (c) Mennucci, E.; Cances, M. T.; Tomasi, J. *J. Phys. Chem. B* **1997**, *101*, 10506. (d) Tomasi, J.; Mennucci, B.; Cances, E. *J. Mol. Struct.: THEOCHEM* **1999**, *464*, 211.
(27) Adamo, C.; Barone, V. *J. Chem. Phys.* **1998**, *108*, 664−675.
(28) Dunning, T. H., Jr. *J. Chem. Phys.* **1989**, *90*, 1007−1023.
(29) Woon, D. E.; Dunning, T. H., Jr. *J. Chem. Phys.* **1993**, *98*, 1358−1371.
(30) Frisch, M. J.; Trucks, G. W.; Schlegel, H. B.; Scuseria, G. E.; Robb, M. A.; Cheeseman, J. R.; Scalmani, G.; Barone, V.; Mennucci, B.; Petersson, G. A.; Nakatsuji, H.; Caricato, M.; Li, X.; Hratchian, H. P.; Izmaylov, A. F.; Bloino, J.; Zheng, G.; Sonnenberg, J. L.; Hada, M.; Ehara, M.; Toyota, K.; Fukuda, R.; Hasegawa, J.; Ishida, M.; Nakajima, T.; Honda, Y.; Kitao, O.; Nakai, H.; Vreven, T.; Montgomery, J. A., Jr.; Peralta, J. E.; Ogliaro, F.; Bearpark, M.; Heyd, J. J.; Brothers, E.; Kudin, K. N.; Staroverov, V. N.; Kobayashi, R.; Normand, J.; Raghavachari, K.; Rendell, A.; Burant, J. C.; Iyengar, S. S.; Tomasi, J.; Cossi, M.; Rega, N.; Millam, J. M.; Klene, M.; Knox, J. E.; Cross, J. B.; Bakken, V.; Adamo, C.; Jaramillo, J.; Gomperts, R.; Stratmann, R. E.; Yazyev, O.; Austin, A. J.; Cammi, R.; Pomelli, C.; Ochterski, J. W.; Martin, R. L.; Morokuma, K.; Zakrzewski, V. G.; Voth, G. A.; Salvador, P.; Dannenberg, J. J.; Dapprich, S.; Daniels, A. D.; Farkas, Ö.; Foresman, J. B.; Ortiz, J. V.; Cioslowski, J.; Fox, D. J. *Gaussian 09*, Revision A.02; Gaussian, Inc.: Wallingford, CT, 2009.